

Reconciling Kaplan and Chinchilla Scaling Laws

Tim Pearce
Microsoft Research

Jinyeop Song
MIT

Abstract

Kaplan et al. [2020] (‘Kaplan’) and Hoffmann et al. [2022] (‘Chinchilla’) studied the scaling behavior of transformers trained on next-token language prediction. These studies produced different estimates for how the number of parameters (N) and training tokens (D) should be set to achieve the lowest possible loss for a given compute budget (C). Kaplan: $N_{\text{optimal}} \propto C^{0.73}$, Chinchilla: $N_{\text{optimal}} \propto C^{0.50}$. This note finds that much of this discrepancy can be attributed to Kaplan counting non-embedding rather than total parameters, combined with their analysis being performed at small scale. Simulating the Chinchilla study under these conditions produces biased scaling coefficients close to Kaplan’s. Hence, this note reaffirms Chinchilla’s scaling coefficients, by explaining the cause of Kaplan’s original overestimation.¹

1 Introduction

Kaplan et al. [2020] (‘Kaplan’) and Hoffmann et al. [2022] (‘Chinchilla’) provided two influential studies measuring the impact of scale in large language models (LLMs). Both informed large-scale efforts on how to trade off model parameters (N) and data size (D) for a given compute budget (C), but with conflicting advice. Kaplan’s finding that $N_{\text{optimal}} \propto C^{0.73}$, $D_{\text{optimal}} \propto C^{0.27}$ led to the conclusion that “*big models may be more important than big data*”, and LLMs trained in the ensuing years committed more resources to model size and less to data size. The subsequent Chinchilla study found $N_{\text{optimal}} \propto C^{0.50}$, $D_{\text{optimal}} \propto C^{0.50}$, leading to their main thesis “*for many current LLMs, smaller models should have been trained on more tokens to achieve the most performant model*”, sparking a trend towards LLMs of more modest model sizes being trained on more data.

What was the cause of the difference in these scaling coefficient estimates that led to vast amounts of compute (plus emissions and finances) being used inefficiently? There have been suggestions that differences could be explained by different optimization schemes [Hoffmann et al., 2022] or datasets [Bi et al., 2024]. This note finds these suggestions incomplete, and offers a simple alternative explanation; much of the discrepancy can be attributed to Kaplan counting non-embedding rather than total parameters, combined with their analysis being performed at small scale.

Set up. Kaplan studied relationships in terms of non-embedding parameters ($N_{\setminus E}$) and non-embedding compute ($C_{\setminus E}$), excluding the linear layers embedding the vocabulary and position indices (N_E). By contrast, Chinchilla studied total parameters (N_T) and total compute (C_T). Define,

$$N_T = N_E + N_{\setminus E}, \quad (1)$$

$$N_E = (h + v)d, \quad (2)$$

where d is dimension of the transformer residual stream, v is vocab size, h is context length (only included when positional embeddings are learned). Using the common approximation for FLOPs $C = 6ND$, we define total and non-embedding compute,

$$C_T = 6N_T D = 6(N_E + N_{\setminus E})D, \quad (3)$$

$$C_{\setminus E} = 6N_{\setminus E} D. \quad (4)$$

The estimated scaling coefficients can be more precisely written (using * to signify ‘optimal’),

$$\text{Kaplan: } N_{\setminus E}^* \propto C_{\setminus E}^{0.73}, \quad (5)$$

$$\text{Chinchilla: } N_T^* \propto C_T^{0.50}. \quad (6)$$

¹Code for Section 2 available: https://github.com/TeaPearce/Reconciling_Kaplan_Chinchilla_Scaling_Laws

Approach overview. Our approach uses information and data from the Chinchilla and Kaplan studies to estimate the scaling laws that would emerge if the Chinchilla relationship had been expressed in terms of $N_{\setminus E}$ & $C_{\setminus E}$, and this had been done at the smaller model sizes used in Kaplan.

We will see that for large N_T , N_E becomes a negligible portion of the model’s parameters and compute cost. Hence in the large parameter regime the two coefficients directly conflict with each other. At smaller values of N_T , N_E is *not* negligible (this is the regime considered in Kaplan’s study – 768 to 1.5B parameters). We find that at the smaller end of this range, the relationship between $N_{\setminus E}^*$ & $C_{\setminus E}$ is not in fact a power law. However, fitting a “local” power law at this small scale, produces a coefficient that is close to Kaplan’s, and hence reconciles these two results.

Our approach in Section 2 is broken down as follows.

- **Step 1.** Fit a suitable function predicting $N_{\setminus E}$ from N_T .
- **Step 2.** Incorporate this function into a model predicting loss in terms of N_T & C_T .
- **Step 3.** Analytically derive the relationship between $N_{\setminus E}^*$ & $C_{\setminus E}$.
- **Step 4.** Simulate synthetic data from the loss model over the model sizes used Kaplan. Fit a local power law for $N_{\setminus E}^*$ in terms of $C_{\setminus E}$.

(Note that whilst this work focuses on the scaling coefficient for parameters, by subscribing to $C = 6ND$ the data coefficient is implied; $N \propto C^a \implies C/D \propto C^a \implies D \propto C^{1-a}$.)

Finally we empirically verify our analysis in Section 3, by training a set of language models at tiny scale and conducting scaling law analyses under various settings. We find that simply changing the basis N_T to $N_{\setminus E}$ produces coefficients inline with Chinchilla and Kaplan respectively, while multiple token budgets and decay schedules does not.

2 Analysis

This Section presents our main analysis. We show that a *local* scaling coefficient of 0.74 to 0.78 (close to Kaplan’s 0.73) can arise when computed in terms of non-embedding parameters in the small-parameter regime, whilst being consistent with Chinchilla’s coefficient.

Step 1. *Fit a suitable function predicting $N_{\setminus E}$ from N_T .*

We require a suitable function relating non-embedding and total parameters. We propose to use the form

$$N_T = N_{\setminus E} + \gamma N_{\setminus E}^{1/3}, \quad (7)$$

for some constant $\gamma > 0$. Aside from having several nice properties (strictly increasing and $\lim_{N_T \rightarrow \infty} N_T = N_{\setminus E}^2$), it can be motivated from both the Kaplan and Chinchilla study.

Kaplan perspective. Consider Kaplan’s method for parameter counting,

$$N_T = 12ld^2 + N_E, \quad (8)$$

where l is number of layers. Whilst Kaplan do not list their model configurations, they do study varying aspect ratio $A = d/l$ for a fixed size model. They find that models of a given size perform similarly over a range of aspect ratios, and range is not affected by model scale (their Figure 5). Hence, we could assume a sizing scheme with fixed aspect ratio ($A \approx 40$ appears sensible from their plots). Assuming this sizing allows us to state,

$$N_T = \frac{12}{A}d^3 + N_E. \quad (9)$$

Observing that $N_{\setminus E} = (12/A)d^3 \implies d = (N_{\setminus E}(A/12))^{1/3}$, and combining with $N_E = (v+h)d$,

$$N_T = N_{\setminus E} + (v+h) \left(\frac{A}{12} \right)^{1/3} N_{\setminus E}^{1/3}. \quad (10)$$

This is the same form as Eq. 7 with $\gamma = (v+h) \left(\frac{A}{12} \right)^{1/3}$.

²**Proof.** $N_T = N_{\setminus E} + \gamma N_{\setminus E}^{1/3} \implies N_T/N_{\setminus E} = 1 + \gamma N_{\setminus E}^{-2/3}$. Examining the r.h.s., $\lim_{N_T \rightarrow \infty} 1 + \gamma N_{\setminus E}^{-2/3} = 1$, hence we conclude on the l.h.s $\lim_{N_T \rightarrow \infty} N_{\setminus E}/N_T = 1$ or $N_{\setminus E} = N_T$.

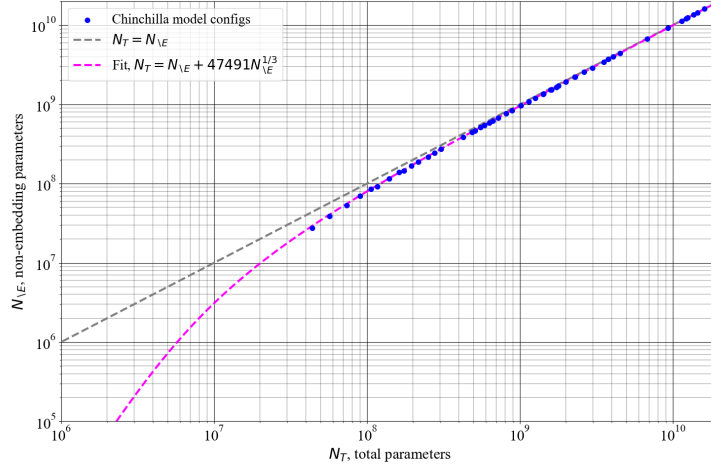


Figure 1: Total parameter count vs. non-embedding parameter count for the suite of models sizes used in the Chinchilla study, along with our fitted approximation. Note the curvature at model sizes below around 200M parameters.

Chinchilla perspective. We empirically fit a function $N_T = N_{\setminus E} + \gamma N_{\setminus E}^\delta$ (note the learnable exponent) to the Chinchilla model configurations listed in Table A9 of Hoffmann et al. [2022] for a range of N_T (44M to 16B). We compute N_E from Eq. 2, using the reported vocab size of 32,000, but ignore the context length 2,048 since Chinchilla used non-learnable position embeddings (though their inclusion effects coefficients only slightly).

Figure 1 shows the configurations and relationship from a model fitted with numpy’s `polyfit`, which produces coefficients, $\gamma = 47491$ & $\delta = 0.34$. The exponent has come out close to 1/3, and an implied aspect ratio $A = 39.2$ (inferred from γ). Hence, this further supports the form in Eq. 7.

Step 2. Incorporate this function into a model predicting loss in terms of N_T & C_T .

Recall that whilst we are interested in the dependence of N_T^* on C_T , this arises only via their mutual relationship with loss

$$N_T^* = \underset{N_T \text{ s.t. } C_T=6N_T D}{\operatorname{argmin}} \operatorname{Loss}(N_T, C_T). \quad (11)$$

In order to analytically study their scaling relationship, we need an analytical form of loss. A functional form central to the Chinchilla study is

$$\operatorname{Loss}(N_T, D) = \frac{N_c}{N_T^\alpha} + \frac{D_c}{D^\beta} + E, \quad (12)$$

$$\operatorname{Loss}(N_T, C_T) = \frac{N_c}{N_T^\alpha} + \frac{D_c}{(C_T/6N_T)^\beta} + E, \quad (13)$$

where $N_c, D_c, \alpha, \beta > 0$ are constants, D is number of training tokens, E is the “unpredictable” loss of the sequence. By differentiating and setting to zero, then rearranging in terms of N_T we find

$$N_T^* = \left(\frac{\alpha N_c}{\beta D_c} \right)^{\frac{1}{\alpha+\beta}} \left(\frac{C_T}{6} \right)^{\frac{\beta}{\alpha+\beta}} \text{ or simply } N_T^* \propto C^{\frac{\beta}{\alpha+\beta}}. \quad (14)$$

We now modify Eq. 13 to be in terms of non-embedding parameters and compute. Note whilst N_T requires Eq. 7 from step 1, the second term avoids this as $D = C_T/6N_T = C_{\setminus E}/6N_{\setminus E}$.

$$\operatorname{Loss}(N_{\setminus E}, C_{\setminus E}) = \frac{N_c}{(N_{\setminus E} + \gamma N_{\setminus E}^{1/3})^\alpha} + \frac{D_c}{(C_{\setminus E}/6N_{\setminus E})^\beta} + E \quad (15)$$

Step 3. Analytically derive the relationship between $N_{\setminus E}^*$ & $C_{\setminus E}$.

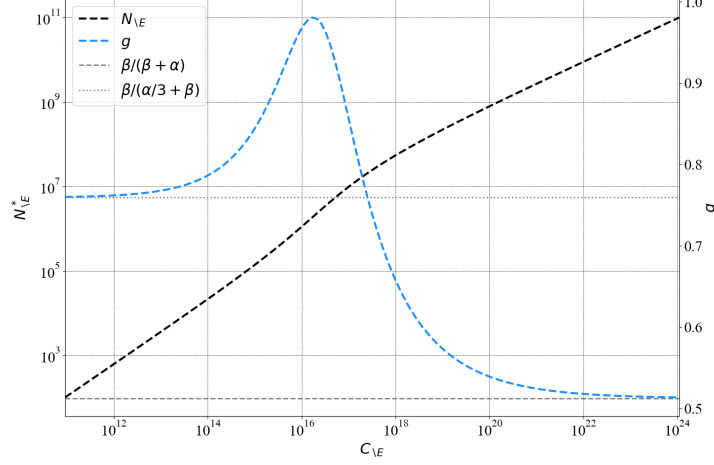


Figure 2: Visualization of Eq. 16 & 17, using the Epoch AI specification.

To find the relationship between $N_{\setminus E}^*$ & $C_{\setminus E}$ we take the derivative of Eq. 15, set to zero and rearrange,

$$6N_{\setminus E}^* \left(N_{\setminus E}^* + \frac{\gamma}{3} N_{\setminus E}^{1/3} \right)^{-\frac{1}{\beta}} \left(N_{\setminus E}^* + \gamma N_{\setminus E}^{1/3} \right)^{\frac{1+\alpha}{\beta}} \left(\frac{\beta D_c}{\alpha N_c} \right)^{\frac{1}{\beta}} = C_{\setminus E}. \quad (16)$$

This shows that in general the relationship between $N_{\setminus E}^*$ & $C_{\setminus E}$ is *not* a power law. However, we can consider a “local” power law approximation. That is, for some particular value of $N_{\setminus E}$, there is some constant g giving a first order approximation (denoted by \asymp) $N_{\setminus E}^* \asymp C_{\setminus E}^g$, where g is defined

$$\frac{1}{g} := \frac{d \log(C_{\setminus E})}{d \log(N_{\setminus E}^*)} = 1 - \frac{1}{\beta} \frac{N_{\setminus E}^{2/3} + \frac{\gamma}{9}}{N_{\setminus E}^{2/3} + \frac{\gamma}{3}} + \frac{\alpha + 1}{\beta} \frac{N_{\setminus E}^{2/3} + \frac{\gamma}{3}}{N_{\setminus E}^{2/3} + \gamma}. \quad (17)$$

Figure 2 plots Eq. 16 and 17, using coefficients for α, β, N_c, D_c from the Epoch AI specification (see later), and $\gamma = 47491$. There are three phases.

- At small scale, $\lim_{N_{\setminus E}^* \rightarrow 0} \frac{1}{g} = \frac{\alpha/3 + \beta}{\beta} \implies N_{\setminus E}^* \asymp C_{\setminus E}^{\frac{\beta}{\alpha/3 + \beta}} 3$.
- At large scale, $\lim_{N_{\setminus E}^* \rightarrow \infty} \frac{1}{g} = \frac{\alpha + \beta}{\beta} \implies N_{\setminus E}^* \asymp C_{\setminus E}^{\frac{\beta}{\alpha + \beta}} 4$, as in the N_T case in Eq. 14.
- There is also a transition phase, where g briefly increases. This happens in between the two limits, when $N_{\setminus E}^{2/3}$ is of the same order as γ . Indeed at exactly the point $N_{\setminus E}^{2/3} = \gamma$, we have $N_T = N_{\setminus E} + \gamma N_{\setminus E}^{1/3} = N_T = 2N_{\setminus E}$, or a 50/50 split between embedding and non-embedding parameters. In Figure 2 we see this transition region occurs around this point; $N_{\setminus E} = \gamma^{3/2} = 47491^{3/2} \approx 1 \times 10^7$.

Step 4. Simulate synthetic data from the loss model over the model sizes used Kaplan. Fit a local power law for $N_{\setminus E}^*$ in terms of $C_{\setminus E}$.

By reading g off Figure 2, we could estimate a local power law and hence scaling coefficient for a given value of $N_{\setminus E}^*$. However, it’s not clear what $N_{\setminus E}^*$ point value is representative of the Kaplan study. We opt for a more faithful estimation procedure, generating synthetic training curves from Eq. 15 across the *range* of model sizes used in Kaplan, and fit coefficients using models falling on the compute efficient frontier. This will also verifies our analytic expression for $N_{\setminus E}^*$ & $C_{\setminus E}$ in Eq. 16.

³**Proof.** As $N_{\setminus E}^* \rightarrow 0$, we can ignore $N_{\setminus E}^*$ terms and $1/g = 1 - (1/\beta)(3/9) + (\alpha + 1)/3\beta = 1 + \alpha/3\beta$.

⁴**Proof.** As $N_{\setminus E}^* \rightarrow \infty$, we can ignore γ terms and $1/g = 1 - (1/\beta) + (\alpha + 1)/\beta = 1 + \alpha/\beta$.

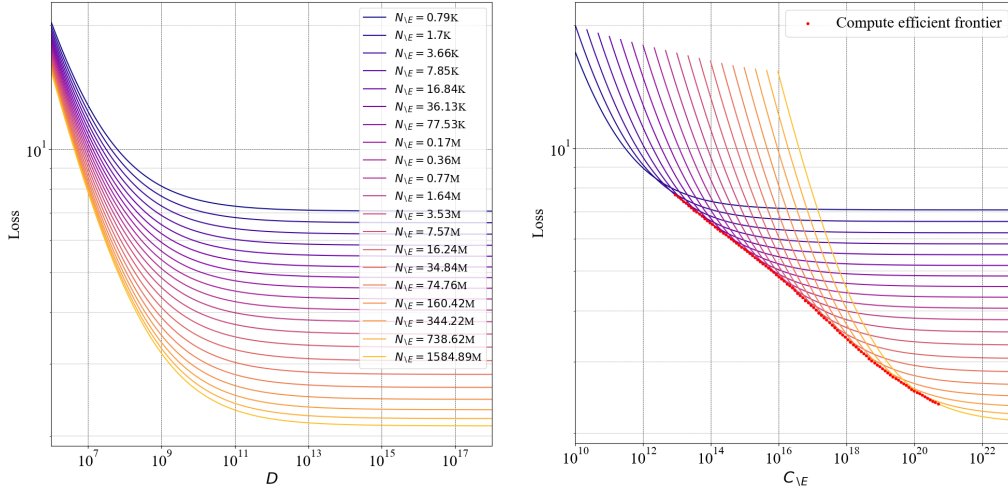


Figure 3: Synthetic training curves from Eq. 15 using the Epoch AI specification, across 20 logarithmically-spaced models matching Kaplan’s size range. Left in terms of training tokens, right in terms of compute.

Figure 3 shows the synthetic training curves generated. We simulated 20 models with $N_{\setminus E}$ ranging from 790 parameters to 1.58B (Kaplan reports using model sizes “ranging in size from 768 to 1.5 billion non-embedding parameters”). For other constants in Eq. 15, there are two options. Whilst the original Chinchilla study reported finding constants of $N_c = 406.4, Dc = 410.7, \alpha = 0.3392, \beta = 0.2849, E = 1.6934 \implies N_T^* \propto C_T^{0.46}$ (‘Chinchilla specification’), Besiroglu et al. [2024] conducted a re-analysis, arguing that the following set of constants were more accurate $N_c = 482.01, Dc = 2085.43, \alpha = 0.3478, \beta = 0.3658, E = 1.8172 \implies N_T^* \propto C_T^{0.51}$ (‘Epoch AI specification’). Our figures adopt the Epoch AI specification and $\gamma = 47491$, though we report final results for the Chinchilla specification also.

Main result. Figure 4 shows the estimated scaling coefficient when fitting a power law to the compute optimal frontier (Chinchilla’s Method 1) produced by these synthetic training curves. This marks our main result – beginning from a model taken from Chinchilla’s study, and modifying two aspects to align with Kaplan’s study ($N_T \rightarrow N_{\setminus E}$, small model sizes 0.79k – 1.58B parameters), we find *local* scaling coefficients,

$$\text{Epoch AI specification: } N_{\setminus E}^* \propto C_{\setminus E}^{0.78}, \quad (18)$$

$$\text{Chinchilla specification: } N_{\setminus E}^* \propto C_{\setminus E}^{0.74}, \quad (19)$$

which are close to the Kaplan coefficient of 0.73.

3 Experiments

We provide brief experiments verifying that our claims hold for models trained at small scale (millions of parameters).

Experiment 1. Firstly, we verify whether scaling coefficients come out close to Chinchilla’s and Kaplan’s when using N_T and $N_{\setminus E}$ respectively.

We trained five models of sizes, $N_T \in [0.8M, 1.6M, 2.1M, 3.3M, 4.6M]$ on the BookCorpus dataset. We used the GPT-2 tokenizer with vocab size of 50,257, and a context length of 16 (whilst much smaller than typical, our experiments suggest scaling coefficients are not affected by context length). Chinchilla’s Method 1 was used to fit scaling coefficients, with the approximation $C = 6ND$.

Models were trained for updates $\in [4000, 4000, 4000, 8000, 8000]$, batchsize was 65,536 tokens per update, for total training tokens $D \in [262M, 262M, 262M, 524M, 524M]$. The best learning rate for each model size was chosen $\in [0.001, 0.005, 0.01, 0.05]$ and no annealing was applied.

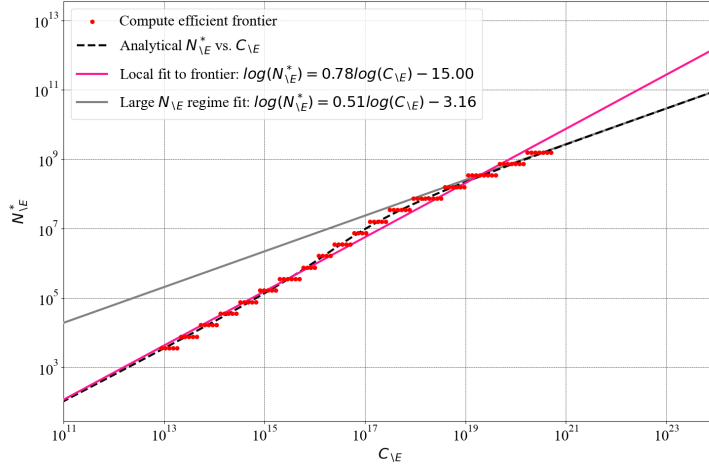


Figure 4: Using synthetic training curves generated in Figure 3, we empirically fit the frontier of compute efficient models using Chinchilla’s Method 1. This gives our main result; synthetic training curves generated from Chinchilla’s study, produce a local scaling coefficient $N_{\setminus E}^* \propto C_{\setminus E}^{0.78}$, close to Kaplan’s coefficient of 0.73. The analytical function from Eq. 16 is also verified.

Result 1. Table 1 shows that when coefficients are fitted to N_T , we find $N_T \propto C_T^{0.49}$ and for $N_{\setminus E}$, we find $N_{\setminus E} \propto C_{\setminus E}^{0.74}$. These match closely with the Chinchilla and Kaplan coefficients.

Experiment 2. We provide an ablation of optimization schemes demonstrating that using multiple training budgets per model affects coefficients only marginally (counter to Chinchilla’s explanation).

- Scheme 1. A single learning rate of 0.001 is set for all models. A single model trained per size, and no annealing applied.
- Scheme 2. The best learning rate is chosen per model. A single model trained per size, and no annealing applied. (As in our N_T vs. $N_{\setminus E}$ comparison.)
- Scheme 3. The best learning rate is chosen per model. A single model trained per size, and cosine annealing applied at the update budget. (**Kaplan study used this.**)
- Scheme 4. The best learning rate is chosen per model. Six models trained per size at different budgets $\in [0.25D, 0.5D, 0.75D, 1.0D, 1.5D, 2.0D]$, and cosine annealing applied. (**Chinchilla study used this.**)

Result 2. Table 1 shows that optimization scheme has a smaller impact on scaling coefficients than switching from N_T to $N_{\setminus E}$. Using a single set of models with no annealing (scheme 2) produces the same coefficients as using the more computationally expensive scheme 4. Counter to Chinchilla’s comment that moving from Kaplan’s scheme 3 to scheme 4 would reduce the scaling coefficient, our experiment suggests the opposite is the case, increasing from 0.46 to 0.49. This might explain our slight overestimation of the scaling coefficients in Eq. 18 & 19.

4 Discussion

This note aimed to explain the difference between the Kaplan and Chinchilla scaling coefficients. We found two issues in Kaplan’s study that combined to bias their estimated scaling coefficient; their choice to count only non-embedding parameters, and studying smaller sized model sizes. This means there is curvature in the true relationship between $N_{\setminus E}^*$ & N_T (Figure 4). At larger values of N_T , the embedding parameter counts become negligible, $N_T = N_{\setminus E}$, and differences would not arise. Alternatively, had Kaplan studied relationships directly in terms of N_T , this issue would also not arise, even at this smaller scale (confirmed by our Experiment 1 finding $N_T \propto C_T^{0.49}$ even for $N_T < 5M$).

Why might embedding parameters be expected to contribute to scaling behavior? Although we do not have a definitive answer, several works evidence that embedding parameters capture

meaningful language properties. Word embedding dimensions can be factorized into semantically interpretable factors [Mikolov et al., 2013a,b, Arora et al., 2018], and LLMs learn linear embeddings of space and time across scales [Gurnee and Tegmark, 2024]. Developing such meaningful embedding structures allows LLMs to perform high-level language operations, such as arithmetic [McLeish et al., 2024]. Therefore, if one believes that the embedding layer does more than just "translate" tokens to a vector of the correct dimension, we see no reason to exclude them in the parameter count. A direction for future work is to investigate the *relative* importance of each parameter type (MLP, QKV projections, embeddings etc.), and whether assigning a count of one to each type is correct.

Limitations. We acknowledge several limitations of our analysis. We have aimed to capture the primary ‘first order’ reason for the difference between the Kaplan and Chinchilla scaling coefficients. But there are multiple other differences between the two studies that likely also affect scaling coefficients; datasets (Kaplan used OpenWebText2, Chinchilla used MassiveText), transformer details (Kaplan used learnable position embeddings while Chinchilla’s were fixed, also differing tokenizers, vocabulary sizes), optimization scheme (Kaplan used scheme 3, Chinchilla scheme 4), differences in computation counting (Kaplan used $C = 6ND$, Chinchilla’s Method 1 & 2 used a full calculation). However, our preliminary work suggested these factors impact coefficients in a more minor way.

Table 1: Comparison of different scaling coefficients from our experiments. Note that the change moving from N_T to $N_{\setminus E}$ has a much larger effect than moving between optimization schemes.

Experiment	a where $N_{\text{optimal}} \propto C^a$	b where $D_{\text{optimal}} \propto C^b$
Chinchilla, N_T	0.50	0.50
Kaplan, $N_{\setminus E}$	0.73	0.27
Ablating N_T vs $N_{\setminus E}$		
Ours, N_T & C_T	0.49	0.51
Ours, $N_{\setminus E}$ & $C_{\setminus E}$	0.74	0.26
Ablating optimization scheme		
Ours, N_T , scheme 1, single lr rate, no anneal	0.58	0.42
Ours, N_T , scheme 2, best lr rate, no anneal	0.49	0.51
Ours, N_T , scheme 3, best lr rate, single-cosine anneal	0.46	0.54
Ours, N_T , scheme 4, best lr rate, multi-cosine anneal	0.49	0.51

References

- Sanjeev Arora, Yuanzhi Li, Yingyu Liang, Tengyu Ma, and Andrej Risteski. Linear algebraic structure of word senses, with applications to polysemy. *Transactions of the Association for Computational Linguistics*, 6:483–495, 2018. doi: 10.1162/tacl_a_00034. URL <https://aclanthology.org/Q18-1034>.
- Tamay Besiroglu, Ege Erdil, Matthew Barnett, and Josh You. Chinchilla scaling: A replication attempt. *arXiv preprint arXiv:2404.10102*, 2024.
- Xiao Bi, Deli Chen, Guanting Chen, Shanhuang Chen, Damai Dai, Chengqi Deng, Honghui Ding, Kai Dong, Qiushi Du, Zhe Fu, et al. Deepseek llm: Scaling open-source language models with longtermism. *arXiv preprint arXiv:2401.02954*, 2024.
- Wes Gurnee and Max Tegmark. Language models represent space and time, 2024.
- Jordan Hoffmann, Sebastian Borgeaud, Arthur Mensch, Elena Buchatskaya, Trevor Cai, Eliza Rutherford, Diego de Las Casas, Lisa Anne Hendricks, Johannes Welbl, Aidan Clark, et al. Training compute-optimal large language models. *arXiv preprint arXiv:2203.15556*, 2022.
- Jared Kaplan, Sam McCandlish, Tom Henighan, Tom B Brown, Benjamin Chess, Rewon Child, Scott Gray, Alec Radford, Jeffrey Wu, and Dario Amodei. Scaling laws for neural language models. *arXiv preprint arXiv:2001.08361*, 2020.
- Sean McLeish, Arpit Bansal, Alex Stein, Neel Jain, John Kirchenbauer, Brian R. Bartoldson, Bhavya Kailkhura, Abhinav Bhatele, Jonas Geiping, Avi Schwarzschild, and Tom Goldstein. Transformers can do arithmetic with the right embeddings, 2024.

Tomas Mikolov, Ilya Sutskever, Kai Chen, Greg S Corrado, and Jeff Dean. Distributed representations of words and phrases and their compositionality. In C.J. Burges, L. Bottou, M. Welling, Z. Ghahramani, and K.Q. Weinberger, editors, *Advances in Neural Information Processing Systems*, volume 26. Curran Associates, Inc., 2013a. URL https://proceedings.neurips.cc/paper_files/paper/2013/file/9aa42b31882ec039965f3c4923ce901b-Paper.pdf.

Tomas Mikolov, Wen-tau Yih, and Geoffrey Zweig. Linguistic regularities in continuous space word representations. In Lucy Vanderwende, Hal Daumé III, and Katrin Kirchhoff, editors, *Proceedings of the 2013 Conference of the North American Chapter of the Association for Computational Linguistics: Human Language Technologies*, pages 746–751, Atlanta, Georgia, June 2013b. Association for Computational Linguistics. URL <https://aclanthology.org/N13-1090>.